Mineralogical Magazine (2022), **86**, 920–928
doi:10.1180/mgm.2022.95

CAMBRIDGE UNIVERSITY PRESS

Article

Bolotinaite, ideally $(Na_7\square)(Al_6Si_6O_{24})F{\cdot}4H_2O$, a new sodalite-group mineral from the Eifel palaeovolcanic region, Germany

Nikita V. Chukanov[1,2*], Natalia V. Zubkova[2], Christof Schäfer[3], I.V. Pekov[2,4], Roman Yu. Shendrik[5], Marina F. Vigasina[2], Dmitry I. Belakovskiy[6], Sergey N. Britvin[7], Vasiliy O. Yapaskurt[2] and Dmitry Yu. Pushcharovsky[2]

[1]Institute of Problems of Chemical Physics, Russian Academy of Sciences, Chernogolovka, Moscow region, 142432 Russia; [2]Faculty of Geology, Moscow State University, Vorobievy Gory, 119991 Moscow, Russia; [3]Gustav Stresemann-Strasse 34, 74257 Untereisesheim, Germany; [4]Vernadsky Institute of Geochemistry and Analytical Chemistry, Russian Academy of Sciences, Kosygina str. 19, 119991 Moscow, Russia; [5]Vinogradov Institute of Geochemistry, Siberian Branch of Russian Academy of Sciences, 1a Favorskii St., Irkutsk, 664033, Russia; [6]Fersman Mineralogical Museum of the Russian Academy of Sciences, Leninsky Prospekt 18-2, 119071 Moscow, Russia and [7]Department of Crystallography, St Petersburg State University, Universitetskaya Nab. 7/9, 199034 St Petersburg, Russia

Abstract

The new sodalite-group mineral bolotinaite, ideally $(Na_7\square)(Al_6Si_6O_{24})F{\cdot}4H_2O$, was discovered in a volcanic ejectum of trachitoid sanidinite collected from the In den Dellen (Zieglowski) pumice quarry, Laach Lake (Laacher See) palaeovolcano, Eifel region, Rhineland-Palatinate, Germany. The associated minerals are sanidine, nepheline, annite and zircon. Bolotinaite occurs as isolated interpenetration prismatic twins on (111) up to 1.3 mm long, complex twins, and rare non-twinned rhombic dodecahedra up to 0.2 mm across. The colour of bolotinaite is pale yellow to pinkish coloured, the streak is white and the lustre is vitreous. Weak orange–yellow fluorescence under longwave ultraviolet radiation ($\lambda = 330$ nm) is due to the presence of trace amounts of the $S_2^{\bullet-}$ radical anion. Bolotinaite is brittle, with a Mohs' hardness of 5. No cleavage is observed. The fracture is uneven. D(meas) = 2.27(2) g·cm^{-3}, D(calc) = 2.291 g·cm^{-3}. Bolotinaite is optically isotropic, with $n = 1.488(2)$ ($\lambda = 589$ nm). The chemical composition is (wt.%, electron microprobe, CO_2 determined by quantitative IR spectroscopy analysis, H_2O calculated from the empirical formula with four H_2O molecules per formula unit): Na_2O 18.30, K_2O 3.87, CaO 0.57, Al_2O_3 28.85, SiO_2 37.97, CO_2 1.66, SO_3 1.37, F 1.60, Cl 0.57, 2.22, H_2O 7.21, –O≡(F,Cl) –0.80, total 101.17. The empirical formula is $(Na_{5.92}K_{0.82}Ca_{0.10}H_{0.08})(Si_{6.33}Al_{5.67}O_{24})(SO_4)_{0.17}F_{0.84}Cl_{0.16}(H_2O)_{3.96}(CO_2)_{0.38}$. A high content of H_2O and the presence of CO_2 molecules and H^+ cations as well as trace amounts of $S_2^{\bullet-}$ are confirmed by means of infrared and Raman spectroscopy. The crystal structure was determined using single-crystal X-ray diffraction data and refined to $R = 0.0335$. Bolotinaite is cubic, space group $I\bar{4}3m$, with $a = 9.027(1)$ Å, $V = 735.7(2)$ Å^3 and $Z = 1$. The strongest lines of the powder X-ray diffraction pattern [d, Å (I, %) (hkl)] are: 6.36 (47) (110), 4.502 (10) (200), 3.679 (100) (211), 2.851 (28) (310), 2.603 (29) (222) and 2.126 (18) (330). The mineral is named in honour of the Russian crystallographer and crystal chemist Dr. Nadezhda Borisovna Bolotina (b. 1949).

Keywords: bolotinaite, new mineral, sodalite group, crystal structure, IR spectroscopy, Raman spectroscopy, Laach Lake palaeovolcano, Eifel, Germany

(Received 18 May 2022; accepted 30 July 2022; Accepted Manuscript published online: 10 August 2022; Associate Editor: Juraj Majzlan)

Introduction

Three kinds of sanidinites can be distinguished among rocks of the Laach Lake (Laacher See) palaeovolcano, Eifel region, Rhineland-Palatinate, Germany. Two of them contain voids with haüyne or nosean crystals. The colour of accessory sodalite-group minerals (blue or white/grey) is the most evident distinctive feature of haüyne sanidinite and nosean sanidinite, respectively. These rocks are considered as derivatives of foyaite magmas which are comagmatic with haüyne- and nosean-bearing syenite, respectively (Frechen, 1976). Unlike haüyne sanidinite, nosean sanidinite contains various accessory Mn-, REE-, Th-, U-, Ti-, Nb- and Zr-minerals. Both types of cavernous sanidinites must be distinguished from the void-free sanidinite which is the product of a deep alkali metasomatic transformation of metamorphic host rocks (Frechen, 1947).

An unusual sanidinite ejectum was collected by one of the authors (C.S.) in 2018 in the pyroclastic deposits of the Laach Lake palaeovolcano. It is a cavernous rock containing yellow to pinkish coloured crystals of a sodalite-group mineral enriched in fluorine. Detailed investigation of this mineral has shown that it is a new mineral species. The new mineral bolotinaite, ideally $(Na_7\square)(Al_6Si_6O_{24})F{\cdot}4H_2O$, described in this paper is the first member of the sodalite group containing the F^- anion as a species-defining component. The mineral is named in honour of the outstanding Russian crystallographer and crystal chemist Dr. Nadezhda Borisovna Bolotina (b. 1949), a leading scientific researcher of the Institute of Crystallography of the Russian

*Author for correspondence: Nikita V. Chukanov, Email: chukanov@icp.ac.ru
Cite this article: Chukanov N.V., Zubkova N.V., Schäfer C., Pekov I.V., Shendrik R.Y., Vigasina M.F., Belakovskiy D.I., Britvin S.N., Yapaskurt V.O. and Pushcharovsky D.Y. (2022) Bolotinaite, ideally $(Na_7\square)(Al_6Si_6O_{24})F{\cdot}4H_2O$, a new sodalite-group mineral from the Eifel palaeovolcanic region, Germany. *Mineralogical Magazine* **86**, 920–928. https://doi.org/10.1180/mgm.2022.95

Academy of Sciences, Moscow. Dr. Bolotina is a senior author or co-author of 128 scientific publications in refereed journals, a major part of which are related to structural chemistry, methods of crystal structure analysis (including those of crystals with modulated structures) and relationships between chemical composition, crystal structures and properties of crystalline materials, including minerals of the sodalite and cancrinite groups.

The new mineral and its name (symbol Bltn) have been approved by the Commission on New Minerals, Nomenclature and Classification (CNMNC) of the International Mineralogical Association (IMA2021-088, Chukanov *et al.*, 2022b). The holotype specimen is deposited in the collection of the Fersman Mineralogical Museum of the Russian Academy of Sciences, Moscow, Russia with the catalogue number 97772.

Experimental methods and data processing

In order to obtain an infrared (IR) absorption spectra of bolotinaite and other sodalite-group minerals (used for comparison), powdered samples were mixed with anhydrous KBr, pelletised, and analysed using an ALPHA FTIR spectrometer (Bruker Optics) in the range of 360–3800 cm^{-1} at a resolution of 4 cm^{-1}. 16 scans were collected for each spectrum. The IR spectrum of an analogous pellet of pure KBr was used as a reference.

The Raman spectrum of a randomly oriented bolotinaite grain was obtained using an EnSpectr R532 spectrometer based on an OLYMPUS CX 41 microscope coupled with a diode laser ($\lambda = 532$ nm) at room temperature. The spectra were recorded in the range from 100 to 4000 cm^{-1} with a diffraction grating (1800 gr mm^{-1}) and spectral resolution of ~6 cm^{-1}. The output power of the laser beam was in the range from 5 to 13 mW. The diameter of the focal spot on the sample was 5–10 μm. The back-scattered Raman signal was collected with a 40 × objective; signal acquisition time for a single scan of the spectral range was 1 s, and the signal was averaged over 50 scans. Crystalline silicon was used as a standard.

Electron microprobe analyses (5 spot analyses for Na, K, Ca, Al, Si, S and Cl, and 11 spot analyses for F) were obtained in wavelength dispersive mode (20 kV and 10 nA; the electron beam was rastered to the 5 × 5 μm area to minimise damage of the mineral). Preliminary energy dispersive spectroscopy analyses showed that the contents of other elements with atomic numbers higher than that of beryllium were below detection limits.

CO_2 content was determined using an IR spectroscopic method with an internal standard (Chukanov *et al.*, 2020a). The content of H_2O was calculated from the empirical formula with four H_2O molecules per formula unit.

Powder X-ray diffraction (XRD) data were collected using a Rigaku R-AXIS Rapid II diffractometer (image plate), Co*K*α, 40 kV, 15 mA, rotating anode with the microfocus optics, Debye-Scherrer geometry, $d = 127.4$ mm and exposure = 15 min. The raw powder XRD data were collected using a program suite designed by Britvin *et al.* (2017). Calculated intensities were obtained from single-crystal XRD data by means of the STOE *WinXPOW* v. 2.08 program suite (STOE, 2003) based on the atomic coordinates and unit-cell parameters.

Single-crystal XRD studies were carried out using an Xcalibur S diffractometer equipped with a CCD detector (Mo*K*α radiation). The crystal structure study of bolotinaite was carried out on a crystal of 0.08 × 0.09 × 0.17 mm in size using an Xcalibur S single-crystal diffractometer equipped with a CCD detector. A full sphere of three-dimensional data was collected. Data reduction was performed using *CrysAlisPro* version 1.171.39.46 (Rigaku Oxford Diffraction, 2018). The data were corrected for Lorentz factor and polarisation effect. The crystal structure of bolotinaite was refined using *Jana2006* software package (Petříček *et al.*, 2014) to $R = 0.0335$ for 663 unique reflections with $I > 3\sigma(I)$ in the frame of the space group $I\bar{4}3m$. Crystal data, data collection information and structure refinement details for bolotinaite are given in Table 1.

Table 1. Crystal data, data collection information and structure refinement details for bolotinaite.

Crystal data	
Crystal size (mm)	0.08 × 0.09 × 0.17
Temperature (K)	293(2)
Crystal system, space group, *Z*	Cubic, $I\bar{4}3m$, 1
Unit-cell dimensions (Å)	$a = 9.02280(10)$
V (Å^3)	734.555(14)
Data collection	
Diffractometer	Xcalibur S CCD
Radiation and wavelength (Å)	Mo*K*α; 0.71073
Absorption correction	Multi-scan
θ range (°)	3.19–30.70
Reflections / reflections with $I > 3\sigma(I)$	708/663
Refinement	
Refinement method	full-matrix least-squares on *F*
Number of refined parameters	22
Final *R* indices [$I > 3\sigma(I)$]	$R = 0.0335$, w$R = 0.0473$
R indices (all data)	$R = 0.0363$, w$R = 0.0480$
GoF	1.24
Largest diff. peak and hole, *e*/Å^3	0.55 and −0.61

Results

Occurrence, general appearance and physical properties

Bolotinaite (Fig. 1) occurs in cavities of a volcanic ejectum of trachitoid sanidinite collected in the In den Dellen (Zieglowski) pumice quarry, 1.5 km NE of Mendig, Laach Lake (Laacher See) palaeovolcano, Eifel region, Rhineland-Palatinate, Germany. The associated minerals are sanidine, nepheline, annite and zircon.

Bolotinaite occurs as isolated interpenetration twins on (111) with a pseudo-hexagonal prismatic habit, up to 1.3 mm long and up to 0.3 mm across (Fig. 1a,c,d). Rarely, complex twins with an angle of 109.47° between twinning axes directed along the diagonals of the cubic unit cell (Fig. 1b), repeated diamond-type twins [additional contact twinning of two penetration twins on (111)], and non-twinned rhombic dodecahedra up to 0.2 mm across are observed.

The colour of bolotinaite is pale yellow to almost colourless or pinkish coloured, the streak is white and the lustre is vitreous. Weak orange–yellow fluorescence under longwave ultraviolet radiation ($\lambda = 330$ nm) is observed. The fluorescence is attributed to the presence of trace amounts of the $S_2^{\bullet-}$ radical anion (see below for details).

Bolotinaite is brittle, with a Mohs hardness of 5. No cleavage is observed. The fracture is uneven. Density measured by flotation in heavy liquids (bromoform + heptane) is equal to 2.27(2) g·cm^{-3}. Density calculated using the empirical formula and unit-cell volume refined from single-crystal XRD data equals to 2.291 g·cm^{-3}.

The new mineral is optically isotropic, with $n = 1.488(2)$ ($\lambda = 589$ nm). Under the microscope, bolotinaite is colourless.

Infrared spectroscopy

The assignment of absorption bands in the IR spectrum of bolotinaite (curve *a* in Fig. 2) is as follows.

https://doi.org/10.1180/mgm.2022.95 Published online by Cambridge University Press

Fig. 1. Bolotinaite grains. The field of view widths are 1.0 mm (a), 0.45 mm (b), 0.3 mm (c) and 0.4 mm (d). Photographer: M. Burkhardt; specimen (c) has catalogue number 97772 in the Fersman mineralogical museum, Moscow.

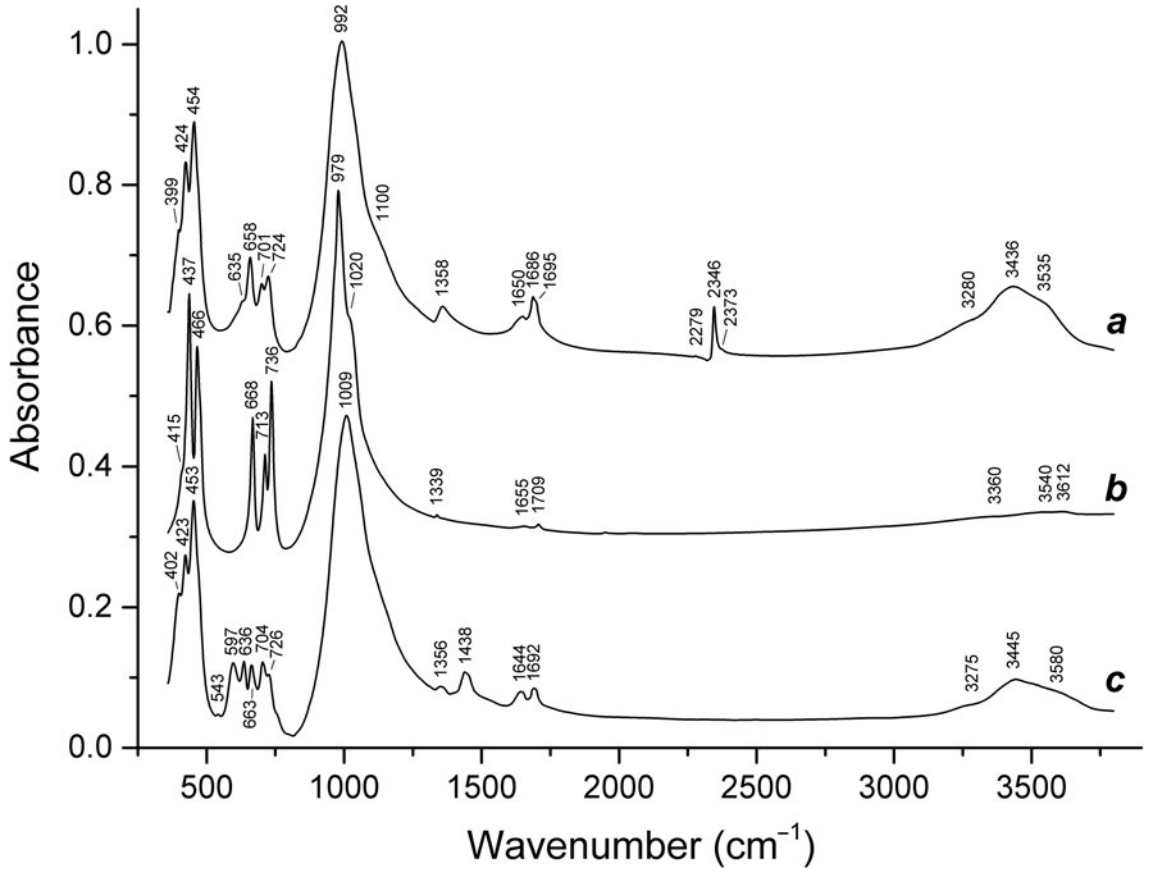

Fig. 2. Powder infrared absorption spectra of (a) bolotinaite, (b) sodalite $Na_{7.98}(Si_{5.80}Al_{6.20}O_{24})Cl_{2.22}$ from the Vishnevogorskiy syenite–miaskite complex, South Urals, Russia (Nishanbaev *et al.*, 2016) and (c) synthetic F-rich sodalite-type compound $Na_{7.38}(Si_{6.74}Al_{5.26}O_{24})(AlF_6)_{0.70}(CO_3)_x{\cdot}nH_2O$ synthesised hydrothermally (at $T = 650$°C, $P = 2$ kBar) in a Si–Al–Na–F–H_2O system (Yakubovich *et al.*, 2011). The spectra are offset for comparison.

https://doi.org/10.1180/mgm.2022.95 Published online by Cambridge University Press

The range of 3200–3600 cm^{-1} is attributed to O–H stretching vibrations; 2373 (weak) and 2346 cm^{-1} to asymmetric stretching vibrations of $^{12}CO_2$ molecules; 2279 (weak) cm^{-1} to asymmetric stretching vibrations of $^{13}CO_2$ molecules; and the range of 1650–1700 cm^{-1} to bending vibrations of H_2O molecules.

The band at 1358 cm^{-1} is, presumably, due to vibrations of the H^+ cation which forms a very strong bifurcated hydrogen bond but does not form covalent bonds (Chukanov, 2014). According to quantum-chemical calculations and single-crystal X-ray structural data, such a situation can be realised in hydrated proton complexes with Zundel- or Eigen-like configurations (see Chukanov *et al.*, 2022a and references therein). Structural data for bolotinaite confirm this assignment (see below).

The 1100 cm^{-1} (shoulder) band is attributed to asymmetric stretching vibrations of the SO_4^{2-} anion; 992 cm^{-1} to stretching vibrations of the aluminosilicate framework; the range of 650–730 cm^{-1} to mixed vibrations of the aluminosilicate framework; and 635 cm^{-1} (shoulder) to bending vibrations of the SO_4^{2-} anion.

Below 500 cm^{-1} bands are attributed to lattice modes involving bending vibrations of the aluminosilicate framework and libration vibrations of H_2O molecules.

The IR spectrum of bolotinaite differs from the IR spectrum of sodalite (curve *b* in Fig. 2) by the presence of rather strong bands of the H_2O and CO_2 molecules, as well as shoulders at 1100 and 635 cm^{-1} corresponding to admixed SO_4^{2-} anions.

The bands of Al–F stretching vibrations observed at 597 and 636 in the IR spectrum of the synthetic F-rich sodalite-type compound $Na_{7.38}(Si_{6.74}Al_{5.26}O_{24})(AlF_6)_{0.70}(CO_3)_x{\cdot}nH_2O$ (Yakubovich *et al.*, 2011: curve *c* in Fig. 2) are absent in the IR spectrum of bolotinaite. This confirms the conclusion that fluorine occurs in bolotinaite as the F^- anion (see structural data below).

Raman spectroscopy

The assignment of absorption bands in the Raman spectrum of bolotinaite (Fig. 3) is as follows.

The band at 3540 cm^{-1} is assigned to H_2O stretching vibrations; 1381 and 1271 cm^{-1} to CO_2 Fermi resonance; 1350 cm^{-1} to, presumably, vibrations of a hydrated proton complex (see above); 1074 cm^{-1} (weak) to stretching vibrations of the aluminosilicate framework or HF librational mode; and 986 cm^{-1} to stretching vibrations of the aluminosilicate framework and symmetric stretching mode of SO_4^{2-}.

The bands at 673 cm^{-1} (weak) and 548 cm^{-1} (weak) are assigned to mixed vibrations of the framework; 580 cm^{-1} (weak) and 605 cm^{-1} (weak) to stretching vibrations of the $S_2^{\bullet-}$ radical anion; 441 cm^{-1} to O–S–O and/or O–Si(Al)–O bending vibrations; and the two bands 283 cm^{-1} (shoulder) and 210 cm^{-1} are due to a combination of low-frequency lattice modes.

Thus, the presence of excessive hydrogen is confirmed in both IR and Raman spectra, which demonstrate bands of free H^+ cations. Bands of CO_3^{2-} are not observed in the Raman spectrum of bolotinaite. Strong luminescence observed under the laser beam at >800 cm^{-1} may be due to the presence of trace amounts of the $S_2^{\bullet-}$ radical anions.

Chemical data

Analytical data are given in Table 2. As noted above, the contents of other elements with atomic numbers higher than that of beryllium are below detection limits. This conclusion is in accordance with IR and Raman spectroscopy data.

The empirical formula based on 12(Si + Al) and $4H_2O$ per formula unit is $(Na_{5.92}K_{0.82}Ca_{0.10}H_{0.08})(Si_{6.33}Al_{5.67}O_{24})(SO_4)_{0.17}F_{0.84}Cl_{0.16}(H_2O)_{3.96}(CO_2)_{0.38}$. The simplified formula is $(Na,K,\square,Ca,H)_8[(Si,Al)_{12}O_{24}][F,(SO_4),Cl]{\cdot}4[(H_2O),(CO_2)]$. The ideal formula of bolotinaite corresponds to the end-member composition $(Na_7\square)(Al_6Si_6O_{24})F{\cdot}4H_2O$.

The Gladstone-Dale compatibility index $1 - (K_p/K_c)$ (Mandarino, 1981) is equal to –0.009 (rated as superior) with

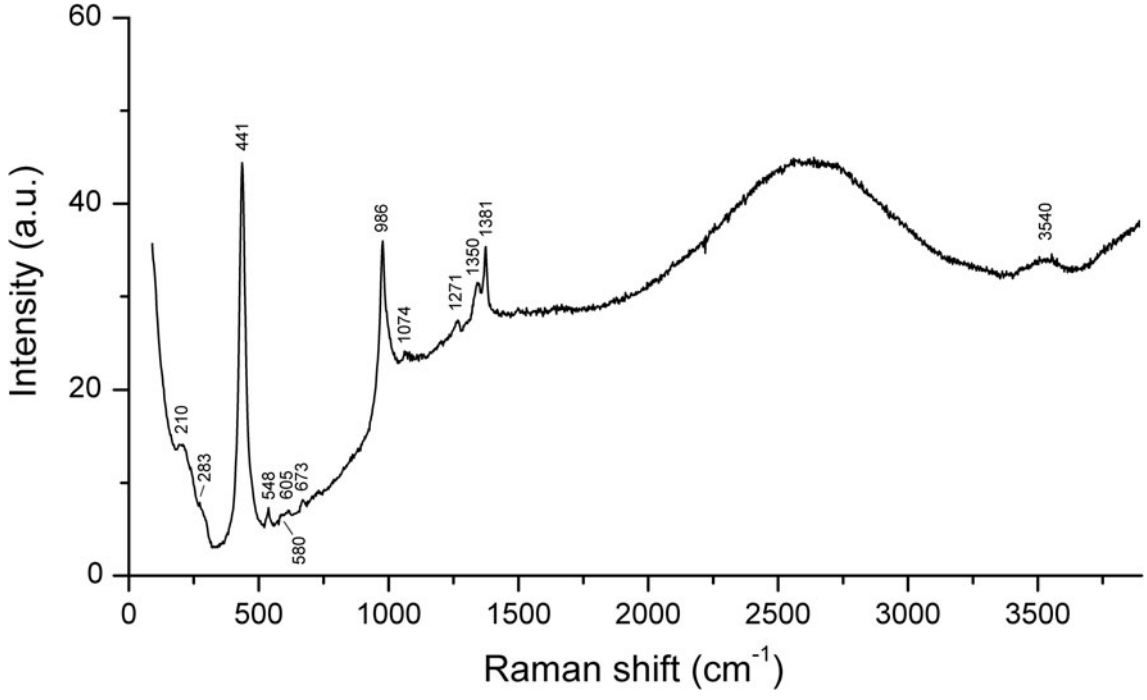

Fig. 3. Raman spectrum of bolotinaite.

https://doi.org/10.1180/mgm.2022.95 Published online by Cambridge University Press

Table 2. Chemical composition of bolotinaite.

Constituent	Wt.%	Range	S.D.	Standard
Na_2O	18.30	18.07–18.52	0.14	Albite
K_2O	3.87	3.75–3.99	0.08	Sanidine
CaO	0.57	0.48–0.66	0.06	Wollastonite
Al_2O_3	28.85	28.73–29.23	0.19	Albite
SiO_2	37.97	37.56–38.27	0.19	SiO_2
CO_2	1.66*			
SO_3	1.37	1.20–1.51	0.13	FeS_2
F	1.60	1.54–1.66	0.05	CaF_2
Cl	0.57	0.49–0.68	0.08	Scapolite
H_2O	7.21**			
–O≡(F,Cl)	–0.80			
Total	101.17			

*Calculated using the IR spectroscopic method (Chukanov *et al.*, 2020a).
**Calculated with four H_2O molecules per formula unit (see description of the crystal structure).
S.D. – standard deviation

the density calculated using the empirical formula and unit-cell parameters refined from the single-crystal X-ray diffraction data.

X-ray diffraction and crystal structure

Powder X-ray diffraction data of bolotinaite are listed in Table 3. The unit-cell parameters refined from the powder data are: $a = 9.027(1)$ Å and $V = 735.7(2)$ Å^3.

The crystal structure of bolotinaite (Fig. 4, Tables 4 and 5) was refined to $R = 0.0335$ for 663 unique reflections with $I > 3\sigma(I)$ in the space group $I\bar{4}3m$. The selection of the I-group was caused by the systematic absences of reflections with $h + k + l \neq 2n$. The

Table 3. Powder X-ray diffraction data (d in Å) of bolotinaite.

I_{obs}	d_{obs}	I_{calc}*	d_{calc}**	h k l
47	**6.36**	**56**	**6.380**	**110**
10	**4.502**	**7**	**4.511**	**200**
100	**3.679**	**100**	**3.684**	**211**
3	3.188	2	3.190	220
28	**2.851**	**25**	**2.853**	**310**
29	**2.603**	**39**	**2.605**	**222**
6	2.410	9	2.411	321
3	2.255	4	2.256	400
18	**2.126**	**27**	**2.127**	**330**
2	1.924	2	1.924	332
1	1.840	3	1.842	422
7	1.770	11	1.770	510
2	1.648	4	1.647	521
7	1.595	13	1.595	440
4	1.548	8	1.547	530
4	1.504	9	1.504	600
4	1.464	9	1.464	611
1	1.427	1	1.427	620
1	1.393	3	1.392	541
4	1.361	11	1.360	622
2	1.330	4	1.330	631
2	1.303	5	1.302	444
2	1.277	3	1.276	543
4	1.228	12	1.228	721
1	1.207	3	1.206	642
1	1.185	4	1.185	730
2	1.147	3	1.146	732
1	1.129	1	1.128	800

*For the calculated pattern, only reflections with intensities ≥1 are given; **for the unit-cell parameters calculated from single-crystal data. The strongest reflections are marked in boldtype.

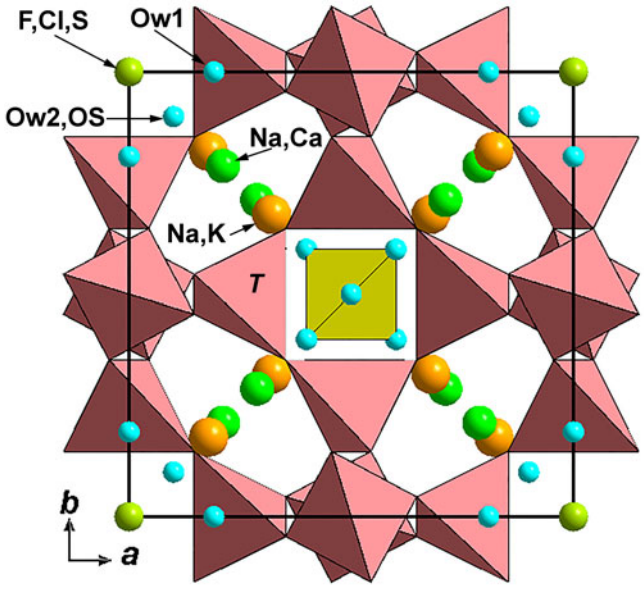

Fig. 4. The crystal structure of bolotinaite (a general view). One SO_4 tetrahedron (yellow) is shown in the centre of the unit cell, other (F,Cl and S) sites are shown as circles. The unit cell is outlined.

measured diffraction pattern contains indications of twinning. The reciprocal lattices of the twin are connected by a 180-degree rotation around one of the spatial diagonals of the cubic cell (Fig. 5). The [111] twin axis is typical for minerals of the sodalite group (Henderson *et al.*, 2000).

The structure of bolotinaite is clearly not centrosymmetric. The mixed positions 8*c* of (Na1, K) and (Na2, Ca) on the spatial diagonals of the unit cell are not located in the inversion centres and are not connected by the inversion centre to each other, differing greatly in occupancy (5.2 atoms and 1.6 atoms, respectively) and nor are they identical by chemical composition.

The sample under study is a twin, the parts of which are connected by a 180-degree rotation about the [111] axis. More precisely, it is a reticular merohedral twin with an index of three. Its reciprocal lattice is arranged in such a way that ⅓ of the lattice sites belong to both twin components, and the remaining ⅔ are equally distributed between the two components. In order to estimate the Flack parameter, albeit formally, but correctly, the inversion matrix must be applied separately to those reflections of one of the twin components that do not overlap with the reflections of the second component. However, there is no such option in the software.

A total of 708 reflections are involved in the refinement of the structural model. Some of them contain contributions from both parts of the twin. For example, the reflection $(0\bar{2}\bar{2})$ from the first component overlaps with the reflection $(\bar{2}\bar{2}0)$ from the second component (see crystallographic information file in Supplementary materials). The total intensity of the diffraction spot is 8040. The reflection $(0\bar{2}2)$ belongs only to the first component and has an intensity of 5586. The reflections $(0\bar{2}\bar{2})$ and $(0\bar{2}2)$ are symmetrically equivalent in the Laue class $m\bar{3}m$, but averaging their intensities to obtain a 'unique' reflection is unacceptable for obvious reasons. For 708 reflections, there are 23 refined parameters with a high data-to-parameter ratio of 30.78. CO_2 molecules were not included in the structure model due to very low occupancy factors of corresponding C and O atoms. However, CO_2 molecules were

https://doi.org/10.1180/mgm.2022.95 Published online by Cambridge University Press

Table 4. Coordinates, equivalent displacement parameters (U_{eq}, in Å^2) of atoms, site multiplicities (Q) and site occupancy factors (s.o.f.) in the structure of bolotinaite.

Site	*x*	*y*	*z*	U_{eq}	*Q*	s.o.f.
T	¼	½	0	0.01159(15)	12	$Si_{0.528}Al_{0.472}$
O1	0.35285(15)	0.35285(15)	0.0445(2)	0.0251(4)	24	$O_{1.00}$
Na,K	0.3209(4)	0.3209(4)	0.3209(4)	0.0619(10)	8	$Na_{0.546}K_{0.1025}$
Na,Ca	0.2117(17)	0.2117(17)	0.2117(17)	0.091(5)	8	$Na_{0.187}Ca_{0.0125}$
F,Cl,S	0	0	0	0.0578(18)*	2	$F_{0.415}Cl_{0.085}S_{0.085}$
Ow1	0.191(2)	0	0	0.058(4)*	12	0.1667
Ow2,OS	0.1006(14)	0.1006(14)	0.1006(14)	0.120(6)	8	$Ow_{0.25}OS_{0.085}$

* U_{iso}

Table 5. Selected interatomic distances (Å) in the structure of bolotinaite.

T–O1	1.6688(14) × 4	S–OS	1.572(12) × 4
Na,Ca–O1	2.349(16) × 3	Na,K–Ow1	2.287(4) × 3
Na,Ca–Ow1	2.708(16) × 3	Na,K–O1	2.527(4) × 3
Na,Ca–O1	3.114(16) × 3	Na,K–Ow2,OS	2.715(13) × 3
Na,Ca–F,Cl	3.309(16)	Na,K–F,Cl	2.798(4)
		Na,K–O1	2.998(4) × 3

undoubtedly determined by IR spectroscopic data and their sites were assumed on the difference-Fourier map (Fig. 6). For this reason, the CO_2 content was included in the formula.

The crystal structure of bolotinaite retains the sodalite-type framework characterised by the presence of four- and six-membered rings of disordered tetrahedra centred by statistically replacing each other's Si and Al atoms. The framework contains so-called sodalite cages which host Na, K and Ca cations, H_2O and CO_2 neutral molecules as well as statistically replacing each other's F^-, Cl^- and SO_4^{2-} anions. The Ow1 and Ow2 sites of oxygen atoms belonging to water molecules were found on the difference-Fourier map. The diffuse shape of these residuals is probably caused by positional disorder of the H_2O sites. The site occupancy factors of the oxygen sites of water molecules were fixed to fit their content of 4 H_2O molecules per formula unit. In accordance with IR and Raman spectroscopy data, sulfur (0.17 S atoms per unit cell) was considered as a part of the sulfate anion and was placed in the mixed (F,Cl,S)-site. Oxygen atoms OS of the SO_4 tetrahedron statistically replace Ow2. The S–OS distance is equal to 1.57 Å.

The O···O distances in pairs of neighbouring water molecules in bolotinaite are OW1···OW1 = 2.40(2) Å and OW2···OW2 = 2.543(19) Å. According to Vyas *et al.* (1978), the shortest O···O distances in hydrated proton complexes are equal to 2.40 and 2.55 Å. *Ab initio* molecular dynamics simulations, with two different electron density functionals, suggest that the shortest O···O

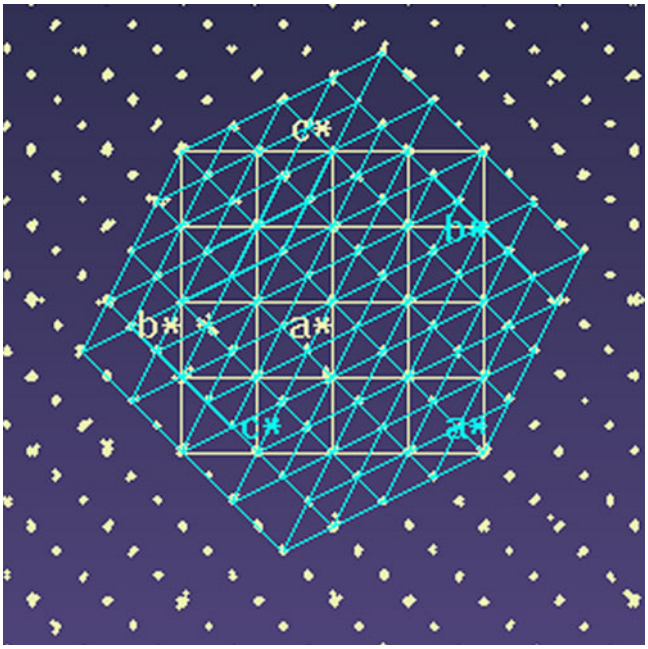

Fig. 5. A fragment of the 3D diffraction pattern of bolotinaite. The pattern is projected along the *a** axis of the reciprocal lattice of the first twin component. Two reciprocal lattices are connected by a 180-degree rotation around the [111] axis in the first lattice.

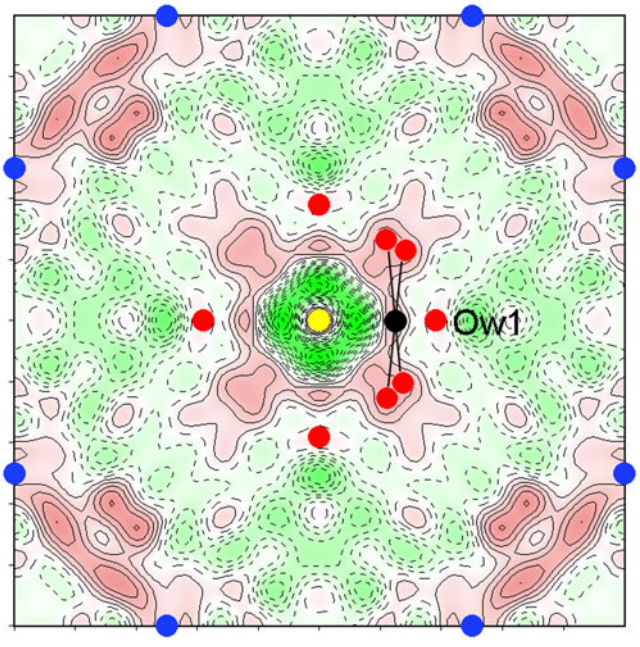

Fig. 6. Residual electron density distribution in the difference Fourier synthesis at $z = 0.5$. The contour intervals are 0.05 e/Å^3. The yellow circle at the centrum of the sodalite cage corresponds to the site predominantly occupied by F with subordinate S and Cl. Black and red circles correspond to C and O atoms, respectively. Central carbon atoms of CO_2 molecules are distributed statistically in the 12*e* position near Ow1. Only two slightly disordered CO_2 molecules with their C atoms at one of twelve sites are shown for simplicity.

https://doi.org/10.1180/mgm.2022.95 Published online by Cambridge University Press

Table 6. Comparative data for bolotinaite and related sodalite-group minerals with the $[Al_6Si_6O_{24}]$ framework having cubic symmetry and the **SOD**-type topology.

Mineral	Bolotinaite	Sapozhnikovite	Sodalite	Nosean	Haüyne	Lazurite
Formula	$(Na_7\square)(Al_6Si_6O_{24})F\cdot_4H_2O$	$Na_8(Al_6Si_6O_{24})(HS)_2$	$Na_8(Al_6Si_6O_{24})Cl_2$	$Na_8(Al_6Si_6O_{24})(SO_4)\cdot H_2O$	$Na_6Ca_2(Al_6Si_6O_{24})(SO_4)_2$	$Na_7Ca(Al_6Si_6O_{24})(SO_4)S_3^-\cdot H_2O$*
Crystal system	Cubic	Cubic	Cubic	Cubic	Cubic	Cubic
Space group	$I\bar{4}3m$	$P\bar{4}3n$	$P\bar{4}3n$	$P\bar{4}3n$	$P\bar{4}3n$	$P\bar{4}3n$
a (Å)	9.0228	8.9146	8.87–8.88	9.05–9.08	9.08–9.13	9.071–9.09
V (Å^3)	734.55	708.45	697.9–700.7	741–749.6	748.6–761.0	746.4–750.3
Z	1	1	1	1	1	1
Strongest lines of the powder X-ray diffraction pattern: d, Å (I, %)	6.36 (47) 3.679 (100) 2.851 (28) 2.603 (29) 2.126 (18) 1.770 (7) 1.595 (7)	6.30 (37) 3.638 (100) 2.821 (14) 2.572 (18) 2.382 (16) 2.101 (29)	6.28 (34) 3.629 (100) 2.808 (10) 2.562 (18) 2.373 (21) 2.092 (34) 1.569 (16)	9.127 (10) 6.464 (36) 3.718 (100) 2.876 (24) 2.625 (49) 2.143 (25) 1.607 (11)	6.47 (16) 3.72 (100) 2.873 (14) 2.623 (25) 2.428 (8) 2.141 (14) 1.781 (10)	6.437 (18) 4.548 (8) 3.711 (100) 2.875 (16) 2.623 (30) 2.142 (16) 1.782 (9)
Optical data	Isotropic n = 1.488	Isotropic n = 1.499	Isotropic n = 1.483–1.487	Isotropic n = 1.461–1.495	Isotropic n = 1.494–1.509	Isotropic n = 1.502–1.522
Density (g·cm^{-3})	2.27 (meas.) 2.264 (calc.)	2.25 (meas.) 2.247 (calc.)	2.27–2.33 (meas.) 2.31 (calc.)	2.25–2.40 (meas.) 2.21 (calc.)	2.44–2.50 (meas.)	2.38–2.45 (meas.) 2.39–2.42 (calc.)
Sources	This work.	Chukanov *et al.* (2021).	Deer *et al.* (1963); Peterson (1983); Hassan and Grundy, (1984); Bokiy and Borutskiy (2003).	Deer *et al.* (1963); Taylor (1967); Hassan and Grundy, (1989); Bokiy and Borutskiy (2003).	Deer *et al.* (1963); Löhn and Schulz, (1968); Burragato *et al.* (1982); Kuribayashi *et al.* (2018).	Deer *et al.* (1963); Hogarth and Griffin (1976); Sapozhnikov (1990); Bokiy and Borutskiy (2003); Chukanov *et al.* (2020b); Sapozhnikov *et al.* (2021a, 2021b).

* The revised formula of lazurite was approved by the IMA–CNMNC on March 2nd, 2021 (Nomenclature Voting proposal 20-H): see Sapozhnikov *et al.* (2021b).

distances in stable Zundel-type $H_5O_2^+$ clusters are 2.44–2.45 and 2.52–2.56 Å (Asthagiri *et al.*, 2005). Subsequently, similar results were obtained in numerous other works reviewed by us recently (Chukanov *et al.*, 2022a). Thus, protonation of a H_2O molecule in bolotinaite should result in the formation of a Zundel-type $H_5O_2^+$ cluster. These data confirm the above conclusion on the occurrence of hydrated proton complexes in bolotinaite, which was made based on IR and Raman spectroscopy and chemical data.

The residual electron density inside the sodalite cage in the difference-Fourier synthesis (Fig. 6) corresponds to linear CO_2 molecules in different orientations, with a central carbon atom near the two-fold axis. Two possible orientations of the CO_2 molecule are shown in Fig. 6. The distance between oxygen atoms in the CO_2 molecule is ~2.33 Å. Residual electron density at the C and O sites assigned to the CO_2 molecules are ~0.16 and ~0.18 $e/Å^3$, respectively. All atoms of the CO_2 molecules occur near the sites of water molecules with the distances of <1 Å from Ow1 and Ow2. Therefore, CO_2 could not be localised directly and were found as a result of the difference-Fourier synthesis.

Discussion

The framework of sodalite-group minerals and topologically related compounds is built involving three kinds of stacking of adjacent layers of Al- and Si-centred tetrahedra, *A*, *B* and *C*, in the stacking sequence $(ABC)_\infty$ (Bonaccorsi and Merlino, 2005; see also Database of Zeolite Structures, http://www.iza-structure.org/databases/). The layers contain six-membered rings of Si- and Al-centred tetrahedra. The unit-cell volume of sodalite-group minerals depends on the content of large extra-framework anions, primarily SO_4^{2-}. In accordance with this regularity, the unit-cell volume of bolotinaite (a mineral with subordinate role of SO_4^{2-}) is intermediate between those of sulfate-free sodalite-group minerals (sodalite and sapozhnikovite) and members of the sodalite group containing SO_4^{2-} as a species-defining component, i.e. haüyne, nosean and lazurite (see Table 6).

Bolotinaite contains trace amounts of the $S_2^{\bullet-}$ radical anion (no more than 0.01 wt.%, according to the luminescence and Raman spectroscopy data), which is a strong yellow chromophore (Ostroumov *et al.*, 2002; Steudel and Chivers, 2019).

The IR spectrum of bolotinaite clearly demonstrates the presence of CO_2 molecules in the mineral. It is important to note that it is impossible to confuse CO_2 in the gas phase and in solids. In the former case, two peaks with close intensities are observed in the range of 2300–2400 cm^{-1} (unresolved rotational structure). In solids, only one strong and narrow peak is observed in this region. In the latter case (i.e. in solids), the presence of a weak isotope satellite peak in the range of 2270–2280 cm^{-1} corresponding to the antisymmetric stretching mode of $^{13}CO_2$ is very indicative. In our spectra, the intensity of the single peak of CO_2 in minerals is two orders stronger than the double peak of atmospheric CO_2.

The state and IR spectra (both powder and single-crystal, including polarisation spectra) of CO_2 molecules in channels of microporous materials and minerals was studied in detail and published in many dozens of papers. In particular, there are many publications related to IR spectroscopy of CO_2 in sodalite- and cancrinite-group minerals. It was shown that a very sharp band at 2351 cm^{-1} in the IR spectra of sodalite and minerals belonging to the haüyne–nosean solid-solution series from Italian palaeovolcanic complexes was assigned unequivocally to the antisymmetric stretching mode of the $^{12}CO_2$ molecule (Bellatreccia *et al.*, 2009). More precise measurements show that the position of this band in the IR spectra of sodalite-group minerals including numerous samples belonging to the haüyne–lazurite solid-solution series (Chukanov *et al.*, 2020a, 2020b; Sapozhnikov *et al.*, 2021a) is in the range of 2340–2343 cm^{-1}. Moreover, the antisymmetric stretching band of $^{12}CO_2$ in sodalite-group minerals from the Somma–Vesuvius volcanic complex, Italy was observed at 2340 cm^{-1} (Balassone *et al.*, 2012). This band is accompanied by a weak peak at 2274 cm^{-1} corresponding to the antisymmetric stretching mode of $^{13}CO_2$. A somewhat lower wavenumber of the IR stretching band of $^{12}CO_2$ (2338 cm^{-1}) was reported for fantappièite and kircherite (Cámara *et al.*, 2010, 2012). Frameworks of these minerals contain both sodalite and Losod cages. The IR spectrum of afghanite from the Ladgvardara gem lazurite deposit, Tajikistan contains a weak and sharp band at 2353 cm^{-1}. The only large cage occurring in this mineral is the liottite cage. Similar bands at 2351 and 2352 cm^{-1} are observed in the IR spectra of holotype samples of farneseite and marinellite (Cámara *et al.*, 2005; Bonaccorsi and Orlandi, 2003), i.e. minerals containing both sodalite and liottite cages.

In the IR spectra of vishnevite and pitiglianoite, i.e. two-layer cancrinite-group minerals with a wide channel, the band for $^{12}CO_2$ is observed at 2351 cm^{-1} (Della Ventura *et al.*, 2005, 2007)

These regularities indicate that the wavenumber of the antisymmetric stretching mode of $^{12}CO_2$ depends on the kind of the host cage or channel: 2340–2343 cm^{-1} for the sodalite cage, 2338 cm^{-1} for the Losod cage and 2351–2353 cm^{-1} for the liottite cage and wide channel of the cancrinite-type framework.

There are a lot of other examples of the presence of CO_2 in zeolite channels of different other minerals with microporous structures (beryl, cordierite, leucite, etc.).

Based on chemical data (in particular, high contents of H_2O, CO_2 and F and the presence of the H^+ cation), one can suppose that bolotinaite crystallised under specific local conditions from a hydrothermal solution enriched in HF and CO_2. Unlike the synthetic F-rich sodalite-type compound with the presumed crystal-chemical formula $Na_{7.38}(Si_{6.74}Al_{5.26}O_{24})(AlF_6)_{0.70}\cdot 4.88H_2O$, synthesised hydrothermally at the temperature of 650°C and pressure of 2 kBar in a Si–Al–Na–F–H_2O system (Yakubovich *et al.*, 2011), bolotinaite does not contain $(AlF_6)^{3-}$ groups (see Fig. 2).

Acknowledgements. The authors are grateful to Rezeda Ismagilova and an anonymous reviewer for the useful discussion. A major part of this work, including chemical and X-ray structural analyses, powder X-ray diffraction, and identification of associated minerals was supported by the Russian Science Foundation, grant No. 22-17-00006. Spectroscopic investigations were carried-out in accordance with the state task of Russian Federation, state registration number AAAA-A19-119092390076-7. The authors thank the X-ray Diffraction Centre of Saint-Petersburg State University for instrumental and computational resources.

Supplementary material. To view supplementary material for this article, please visit https://doi.org/10.1180/mgm.2022.95

Competing interests. The authors declare none.

References

Asthagiri D., Pratt L.R. and Kress J.D. (2005) *Ab initio* molecular dynamics and quasichemical study of $H^+(aq)$. *Proceedings of the National Academy of Sciences of the United States of America*, **102**, 6704–6708.

Balassone G., Bellatreccia F., Mormone A., Biagioni C., Pasero M., Petti C., Mondillo N. and Fameli G. (2012) Sodalite-group minerals from the Somma Vesuvius volcanic complex, Italy: a case study of K-feldspar-rich

xenoliths. *Mineralogical Magazine*, **76**, 191–212. https://doi.org/10.1180/minmag.2012.076.1.191

Bellatreccia F., Della Ventura G., Piccinini M., Cavallo A. and Brilli M. (2009) H_2O and CO_2 in minerals of the haüyne-sodalite group: an FTIR spectroscopy study, *Mineralogical Magazine*, **73**, 399–413. https://doi.org/10.1180/minmag.2009.073.3.399.

Bokiy G.B. and Borutskiy B.E. (editors) (2003) *Minerals*. Vol. V(2): *Framework Silicates*. Moscow, Nauka, 379 pp. [in Russian].

Bonaccorsi E. and Merlino S. (2005) Modular microporous minerals: Cancrinite-davyne group and C–S–H Phases. Pp. 241–290 in: *Micro- and Mesoporous Mineral Phases* (G. Ferraris and S. Merlino, editors). Reviews in Mineralogy & Geochemistry, **57**. Mineralogical Society of America and the Geochemical Society, Washington, DC.

Bonaccorsi E. and Orlandi P. (2003) Marinellite, a new feldspathoid of the cancrinite-sodalite group, *European Journal of Mineralogy*, **15**, 1019–1027. https://doi.org/10.1127/0935-1221/2003/0015-1019

Britvin S.N., Dolivo-Dobrovolsky D.V. and Krzhizhanovskaya M.G. (2017) Software for processing the X-ray powder diffraction data obtained from the curved image plate detector of Rigaku RAXIS Rapid II diffractometer. *Zapiski Rossiiskogo Mineralogicheskogo Obshchestva* (*Proc. Russ. Mineral. Soc.*), **146**, 104–107 [in Russian].

Burragato F., Maras A. and Rossi A. (1982) The sodalite group minerals in the volcanic areas of Latium. *Neues Jahrbuch Monatsheft*, **1982**, 433–445

Cámara F., Bellatreccia F., Della Ventura G. and Mottana A. (2005) Farneseite, a new mineral of the cancrinite-sodalite group with a 14-layer stacking sequence: occurrence and crystal structure. *European Journal of Mineralogy*, **17**, 839–846. https://doi.org/10.1127/0935-1221/2005/0017-0839

Cámara F., Bellatreccia F., Della Ventura G., Mottana A., Bindi L., Gunter M.E. and Sebastiani M. (2010) Fantappièite, a new mineral of the cancrinite-sodalite group with a 33-layer stacking sequence: Occurrence and crystal structure. *American Mineralogist*, **95**, 472–480. https://doi.org/10.2138/am.2010.3279

Cámara F., Bellatreccia F., Della Ventura G., Gunter M.E., Sebastiani M. and Cavallo A. (2012) Kircherite, a new mineral of the cancrinite-sodalite group with a 36-layer stacking sequence: Occurrence and crystal structure, *American Mineralogist*, **97**, 1494–1504. https://doi.org/10.2138/am.2012.4033

Chukanov N.V. (2014) *Infrared Spectra of Mineral Species: Extended Library*. Springer-Verlag GmbH, Dordrecht–Heidelberg–New York–London. 1716 pp.

Chukanov N.V., Vigasina M.F., Zubkova N.V., Pekov I.V., Schäfer C., Kasatkin A.V., Yapaskurt V.O. and Pushcharovsky D.Yu. (2020a) Extra-framework content in sodalite-group minerals: Complexity and new aspects of its study using infrared and Raman spectroscopy. *Minerals*, **10**, 363. https://doi.org/10.3390/min10040363

Chukanov N.V., Sapozhnikov A.N., Shendrik R.Yu., Vigasina M.F. and Steudel R. (2020b) Spectroscopic and crystal-chemical features of sodalite-group minerals from gem lazurite deposits. *Minerals*, **10**, 1042. https://doi.org/10.3390/min10111042

Chukanov N.V., Zubkova N.V., Pekov I.V., Shendrik R.Y., Varlamov D.A., Vigasina M.F., Belakovskiy D.I., Britvin S.N., Yapaskurt V.O. and Pushcharovsky D.Y. (2021) Sapozhnikovite, IMA 2021-030. CNMNC Newsletter 62. *Mineralogical Magazine*, **85**. https://doi.org/10.1180/mgm.2021.62

Chukanov N.V., Vigasina M.F., Rastsvetaeva R.K., Aksenov S.M., Mikhailova Ju.A. and Pekov I.V. (2022a) The evidence of hydrated proton in eudialyte-group minerals based on Raman spectroscopy data. *Journal of Raman Spectroscopy*, **53**, https://doi.org/10.1002/jrs.6343.

Chukanov N.V., Zubkova N.V., Schäfer C., Pekov I.V., Vigasina M.F., Belakovskiy D.I., Britvin S.N., Yapaskurt V.O. and Pushcharovsky D.Y. (2022b) Bolotinaite, IMA 2021-088. CNMNC Newsletter 65. *Mineralogical Magazine*, **86**, 354–358.

Deer W.A., Howie R.A. and Zussman J. (1963) *Rock-forming Minerals. Vol. 4: Framework Silicates*. Longmans, London, pp. 289–302.

Della Ventura G., Bellatreccia F. and Bonaccorsi E. (2005) CO_2 in minerals of the cancrinite-sodalite group: pitiglianoite, *European Journal of Mineralogy*, **17**, 847–851. https://doi.org/10.1127/0935-1221/2005/0017-0847

Della Ventura G., Bellatreccia F., Parodi G.C., Cámara F. and Piccinini M. (2007) Single-crystal FTIR and X-ray study of vishnevite, ideally $[Na_6(SO_4)][Na_2(H_2O)_2](Si_6Al_6O_{24})$, *American Mineralogist*, **92**, 713–721. https://doi.org/10.2138/am.2007.2197

Frechen J. (1947) Vorgänge der Sanidinit-Bildung im Laacher Seegebiet. *Fortschritte der Mineralogie*, **26**, 147–166 [in German].

Frechen J. (1976) Siebengebirge am Rhein, Laacher Vulkangebiet, Maargebiet der Westeifel. *Sammlung geologischer Führer*, **56**, 3. Auflage. Stuttgart, Schweitzerbart, 209 p. [in German].

Hassan I. and Grundy H.D. (1984) The crystal structures of sodalite-group minerals. *Acta Crystallographica*, **B40**, 6–13.

Hassan I. and Grundy H.D. (1989) The structure of nosean, ideally $Na_8[Al_6Si_6O_{24}]SO_4{\cdot}H_2O$. *The Canadian Mineralogist*, **27**, 165–172.

Henderson W.A., Jr, Richards R.P. and Howard D.G. (2000) Elongated twins of sodalite and other isometric minerals. *Mineralogical Record*, 2000, **31**, 141–152.

Hogarth D.D. and Griffin W.L. (1976) New data on lazurite. *Lithos*, **9**, 39–54.

Kuribayashi T., Aoki S. and Nagase T. (2018) Thermal behavior of modulated haüyne from Eifel, Germany: In situ high–temperature single–crystal X–ray diffraction study. *Journal of Mineralogical and Petrological Sciences*, **113**, 51–55.

Löhn J. and Schulz H. (1968) Strukturverfeinerung am gestörten Haüyn, $(Na_5K_1Ca_2)Al_6Si_6O_{24}(SO_4)_{1.5}$, *Neues Jahrbuch für Mineralogie, Abhandlungen*, **109**, 201–210 [in German].

Mandarino J.A. (1981) The Gladstone-Dale relationship. IV. The compatibility concept and its application. *The Canadian Mineralogist*, **41**, 989–1002.

Nishanbaev T.P., Rassomahin M.A., Blinov I.A. and Popova V.I. (2016) Minerals of sodalite-cancrinite pegmatites from the Vishnevogorsk miaskite massif, South Urals. *Mineralogy*, **3**, 40–52 [in Russian].

Ostroumov E., Fritsch E., Faulques E. and Chauvet O. (2002) Etude spectrometrique de la lazurite du Pamir, Tajikistan. *The Canadian Mineralogost*, **40**, 885–893 [in French].

Peterson R.C. (1983) The structure of hackmanite, a variety of sodalite, from Mont St-Hilaire, Quebec. *The Canadian Mineralogist*, **21**, 549–552.

Petříček V., Dušek M. and Palatinus L. (2014) Crystallographic Computing System JANA2006: General features. *Zeitschrift für Kristallographie – Crystalline Materials*, **229**, 345–352.

Rigaku Oxford Diffraction (2018) *CrysAlisPro Software System, v. 1.171.39.46*, Rigaku Corporation, Oxford, UK.

Sapozhnikov A.N. (1990) Indexing of additional reflections on the X-ray Debye diffraction patterns of lazurite concerning the study of modulation of its structure. *Zapiski Vsesoyuznogo Mineralogicheskogo Obshchestva* (*Proceedings of the Soviet Mineralogical Society*), **119**(1), 110–116 [in Russian with English abstract].

Sapozhnikov A.N., Tauson V.L., Lipko S.V., Shendrik R.Yu., Levitskii V.I., Suvorova L.F., Chukanov N.V. and Vigasina M.F. (2021a) On the crystal chemistry of sulfur-rich lazurite, ideally $Na_7Ca(Al_6Si_6O_{24})(SO_4)(S_3)^{-}{\cdot}nH_2O$. *American Mineralogist*, **106**. https://doi.org/10.2138/am-2020-7317.

Sapozhnikov A.N., Chukanov N.V., Shendrik R.Yu., Vigasina M.F., Tauson V.L., Lipko S.V., Belakovskiy D.I., Levitskii V.I., Suvorova L.F. and Ivanova L.A. (2021b) Lazurite: confirmation of the status of mineral species with the formula $Na_7Ca(Al_6Si_6O_{24})(SO_4)S_3^{\bullet-}{\cdot}H_2O$ and new data. *Zapiski Vserossiiskogo Mineralogicheskogo Obshchestva* (*Proceedings of the Russian Mineralogical Society*), **150**(4), 92–102. https://doi.org/10.31857/S0869605521040055 [in Russian with English abstract].

Steudel R. and Chivers T. (2019) The role of polysulfide dianions and radical anions in the chemical, physical and biological sciences, including sulfur-based batteries. *Chemical Society Reviews*, **48**, 3279–3319 and 4338.

STOE (2003) *WinXPow Version 2.08*. STOE & Cie GmbH, Darmstadt, Germany.

Taylor D. (1967) The sodalite group of minerals. *Contributions to Mineralogy and Petrology*, **16**, 172–188.

Vyas N.K., Sakore T.D. and Biswas A.B. (1978) The structure of 4-methyl-5-sulphosalicylic acid tetrahydrate. *Acta Crystallographica*, **B34**, 3486–3488. https://doi.org/10.1107/S0567740878011413

Yakubovich O.V., Kotel'nikov A.R., Shchekina T.I., Gramenitskiy E.N. and Zubkov E.S. (2011) New representative in the sodalite structure type with extraframework anions $[AlF_6]^{3-}$. *Crystallography Reports*, **56**, 190–197.

https://doi.org/10.1180/mgm.2022.95 Published online by Cambridge University Press